

1 **Abstract**

2 Adsorption of two widespread emerging water contaminants (atrazine and paracetamol) onto three
3 different activated carbons was investigated. The carbons were characterized and the influence of their
4 physicochemical properties on the adsorption performance of atrazine and paracetamol was evaluated.
5 The adsorption equilibrium data were fitted to different adsorption isotherm models (Langmuir,
6 Freundlich, and Dubinin-Radushkevich) while the adsorption rates were described using three different
7 kinetic models (pseudo second order, intraparticle diffusion and a new approach based on diffusion-
8 reaction models). The results indicated that hydrophobic character of the compounds does not affect the
9 sorption capacity of the tested carbons but does influence the uptake rate. The model proposed, based on
10 mass balances, lead to interpret and compare the kinetic of different adsorbents in contrast to classical
11 empirical models. The model is a simple and powerful tool able to satisfactorily estimate the sorption
12 capacities and kinetics of the carbons under different operation conditions by means of only two
13 parameters with physical meaning. All the carbons studied adsorbed paracetamol more effectively than
14 atrazine, possibly due to the fact that sorption takes place by H-bonding interactions.

15 **Keywords:** adsorption, paracetamol, atrazine, kinetics, diffusion model, sludge activated carbon

16 **Introduction**

17 The emission of so-called “emerging contaminants” has arisen recently as an environmental problem.
18 This group is mainly composed of compounds used in large quantities in everyday life, such as human
19 and veterinary pharmaceuticals, personal care products, surfactants, pesticides and different industrial
20 additives. Removal of some emerging contaminants in wastewater treatment plants (WWTP) was found
21 to be rather low due to the fact that most of them are resistant to biological degradation. Consequently
22 sewage effluents are one of the main sources of these compounds and their metabolites, which can
23 potentially end up in finished drinking water (Petrovic et al. 2003; de Ridder et al. 2010).

24 One effective way to eliminate these recalcitrant compounds could be to introduce an adsorption
25 step before dumping WWTP effluents. Activated carbons are widely used to adsorb organic substances
26 from gases or liquids. They are commonly obtained from various organic precursors such as bituminous
27 coal, peat, wood, coconut shell (Marsh and Rodriguez-Reinoso, 2006). In recent years, there has been a
28 growing interest in converting organic waste materials with high carbon content into activated carbon
29 (Schröder et al. 2011). Sludge is waste material produced in large volumes in the sewage treatment plants.

1 It can be recycled by composting and used in agricultural land, incinerated or used in landfills. Nowadays,
2 new environmentally benign alternatives for this residue are being sought. In this sense, sewage sludge
3 has been investigated as an attractive precursor for activated carbon production (Smith et al. 2009).

4 The adsorption capacity of an activated carbon depends on its physico-chemical characteristics
5 (e.g. surface area, pore size, functional groups,..) and the nature of the adsorbate (e.g. molecular weight
6 and size, hydrophobicity, polarity, functional groups (Mohamed et al. 2011). In the literature, several
7 solute properties that influence organic solute adsorption onto activated carbon have been discussed.
8 Some authors have tried to directly relate octanol–water coefficient (K_{ow}) to adsorption capacity (De
9 Ridder et al. 2010). A good relation between this property and adsorption was found for most of the
10 hydrophobic contaminants onto activated carbons. However, a poor correlation was shown when the
11 solutes were small and hydrophilic (Westerhoff et al., 2005) or when they were aromatic compounds
12 (Chen et al., 2007). In the case of aromatic compounds several authors have suggested that they can be
13 adsorbed on activated carbons by dispersion interactions between the π -electrons of the aromatic ring and
14 those of the graphene layers (Li et al., 2009). Functionalization of either the adsorbent or the adsorbate
15 profoundly affects these dispersion interactions. On the other hand, if the aromatic compounds
16 have hydrogen-bonding functional groups, hydrogen bonding can contribute to the compound adsorption.
17 (Moreno- Castilla 2004, Terzyk 2000). However, the specific mechanisms, through which adsorption of
18 aromatic compounds occur are still not well established.

19 In this work, we study the adsorption of two widespread water emerging contaminants, atrazine
20 (1,3,5-Triazine-2,4-diamine, 6-chloro-N-ethyl-N'-(1-methylethyl)) and paracetamol (N-acetyl-p-
21 aminophenol) onto different activated carbons prepared from various raw materials: a bituminous coal, a
22 lignite and sewage sludge. To understand interactions between the sorbents and the target contaminants,
23 the texture and chemical properties of active carbons were characterized. This research aims to provide
24 new information for a better understanding of the factors and the mechanism involved in the adsorption
25 process. Moreover, a new kinetic model, based on mass balances and description of transfer processes,
26 has been proposed to describe with physical interpretation the sorption kinetic, overcoming the limitation
27 of classic kinetic empirical models.

28

1 **Material and Methods**

2 Adsorbates

3 The adsorbates used were a pesticide, atrazine (Sigma-Aldrich, Germany) and a pharmaceutical,
4 paracetamol (Fagron, Spain). Table 1 shows physico-chemical properties of these two compounds.

5 Paracetamol stock solution (200 mg/L) was prepared with ultra-pure water (Milli-Q). Atrazine
6 stock solution (1000 mg/L) was prepared with acetone (Scharlau, Spain). From these solutions, samples
7 for calibration and sorption experiments were obtained by dilution.

8 Adsorbents

9 Three activated carbons were evaluated. Two of them were commercial activated carbons. Filtrasorb-400
10 (F-400) was supplied by Chemviron (Belgium) and obtained from a bituminous coal. Norit PK 1-3 (NPK)
11 was produced from peat by Norit Americas Inc. (USA). The third carbon was a sludge-based activated
12 carbon-like material (SBC) prepared from sludge from WWTP through the methodology described by
13 Smith and Fowler (2011).

14 Textural and chemical carbons characterization methods

15 The texture of the three carbons was characterized by N₂ adsorption isotherm at -196 °C, in a
16 conventional volumetric apparatus (ASAP 2420 from Micrometrics). Before each experiment, the samples
17 were outgassed under vacuum at 120°C overnight to remove any adsorbed moisture and/or gases. The N₂
18 isotherms were used to calculate the specific surface area (S_{BET}), total pore volume, (V_{TOT}), at a relative
19 pressure of 0.95, and pore size distribution. The pore size distribution (PSD) was evaluated using the
20 density functional theory (DFT), assuming slit-shape pore geometry.

21 The carbons were further characterized for their elemental analysis using a LECO CHN-2000
22 and a LECO Sulphur Determination S-144-DR. The ash content and humidity were determined according
23 to the methods described in ISO 1171 and ISO 5068.

1 FTIR technique was applied in order to determine the main functional groups on the surface
2 carbons. For this purpose spectra were determined between 4000 and 400 cm^{-1} using an FTIR
3 spectroscope (Spectrum 65 FT-IR, PerkinElmer).

4 Adsorption assays

5 For kinetics studies, 50 mg of adsorbent were added to 250 mL of 40 mg/L atrazine or paracetamol
6 solutions. Mixtures were stirred at 25°C in a multipoint agitation plate. At different times (from 1 to 48
7 hours), samples were taken and filtered through a cellulose acetate filter (0.2 μm diameter pore) and the
8 remaining concentrations were analyzed in a UV/Vis spectrophotometer (Lambda 25 PerkinElmer) at 242
9 nm for paracetamol and 224.9 nm for atrazine. The detection limit for paracetamol was 144 ppb and for
10 atrazine 220 ppb. The paracetamol and atrazine uptake (q_t) was calculated by:

$$11 \quad q_t = \frac{(C_0 - C_t) V}{W} \quad (1)$$

12 Where q_t is the amount (mg/g) of atrazine or paracetamol adsorbed at time t , C_0 is the initial
13 concentration (mg/L), C_t is the concentration at time t (mg/L), V is the volume (L) of the adsorbate
14 solution and W is the weight (g) of carbon used.

15 Equilibrium adsorption studies were made at 25°C varying the atrazine or paracetamol
16 concentration (1-150 mg/L). The remaining atrazine and paracetamol concentrations after equilibrium
17 time were determined as described above and the uptake was calculated using Eq. (1).

18 Adsorption modeling

19 Isotherms experimental data were fitted to two-parameter isotherm models: Langmuir (Eq.2), Freundlich
20 (Eq.3) and Dubinin-Radushkevich (DR) (Eq. 4,5 and 6)

$$21 \quad q_e = \frac{q_{max} K_L C_e}{1 + K_L C_e} \quad (2)$$

$$22 \quad q_e = K_f C_e^{1/n} \quad (3)$$

$$23 \quad \ln q_e = \ln q_{max} - \beta \mathcal{E}^2 \quad (4)$$

$$24 \quad \mathcal{E} = RT \ln (1 + 1/C_e) \quad (5)$$

1
$$E = \frac{1}{\sqrt{2\beta}} \quad (6)$$

2 Where q_e (mg/g) is the amount of compound adsorbed per mass unit of activated carbon, C_e (mg/L) is the
 3 organic compound concentration at equilibrium, q_{max} (mg/g) is the maximum adsorption capacity, K_L
 4 (L/mg) is a constant related to the affinity between the pollutant and the adsorbent, K_f ((mg/g) (L/mg)^{1/n})
 5 is the Freundlich sorption constant and “n” is a constant related to adsorption intensity. \mathcal{E} is the Polanyi
 6 potential, R is the gas universal constant (J/(molK)), T is temperature (K) and β is a constant related to
 7 free energy (E) of adsorption (J/mol) of the adsorbate.

8 Kinetic modeling in sorption processes has been described for different approaches (Clark 1987;
 9 Wolborska 1989; Yan et al. 2001, Ho et al 1998). In the present work, the different kinetic models such as
 10 pseudo-second order (Eq. 7), intraparticle diffusion (Eq. 8), and the diffusion-adsorption model were used
 11 to describe the non-equilibrium stage of adsorption.

12
$$\frac{\partial q_t}{\partial t} = k_2 (q_e - q_t)^2 \quad (7)$$

13
$$q_t = k_p t^{0.5} + A \quad (8)$$

14 Where k_2 (L/(mg min)) is the rate constant, k_p is the intraparticle rate constant (mg/(L·min^{0.5})) and A is
 15 the intercept (mg/L).

16 The diffusion-adsorption model is based on the well-known diffusion-reaction mathematical
 17 model (Cultip and Shacham, 2008) which has been successfully used in a wide range of chemical
 18 engineering related systems (Dorado et al. 2014). The model proposed is based on the following
 19 assumptions:

- 20 1.-Isothermal conditions across the batch system and over time.
- 21 2.-Planar geometry and perpendicular diffusion through the solid are used to derive to the model
 22 equations.
- 23 3.-The aqueous-solid interface resistance is negligible.
- 24 4.-Aqueous-solid interface equilibrium is described by Langmuir’s isotherm, according to previous results
 25 (Tab. 4).

1 5.-There is a maximum penetration depth for the pollutant into the solid phase.

2 Isothermal conditions are needed to define the isotherm equilibrium and they are ensured by
3 means of controlled room temperature. Planar geometry only influences in the coordinate system used for
4 solving the differential equations. The assumption that interface resistance is negligible is consistent with
5 the operation conditions used in the experimental work since an optimal stirring was ensured. Finally, the
6 concept of maximum penetration is employed for comparing the behavior of the system under different
7 conditions and the boundary set is in concordance with the size of the particles.

8 According to the above specifications, the mass balance in the liquid phase can be formulated as:

9
$$\frac{\partial C_t}{\partial t} = -\frac{D * a_s}{\varepsilon_D} \left(\frac{\partial C_s}{\partial x} \right) \Big|_{x=0} \quad (9)$$

10 for the initial conditions: $t=0$, $C_t = C_0$

11 Where D is the diffusion coefficient (m^2/min), a_s is the effective specific surface area (m^2/m^3),
12 ε_D is the fraction of liquid in the total volume, C_s and C_t (mg/L) are organic compound concentrations in
13 the solid and liquid phases, respectively and x is the depth from the sorbent material surface (m).

14 The mass balance in the solid phase is described by the following equation (10)

15
$$\frac{\partial C_s}{\partial t} = -D \left(\frac{\partial^2 C_s}{\partial x^2} \right) \quad (10)$$

16 With the following boundary conditions:

17
$$at \ x = 0, \quad C_s = \frac{q_{max} k_L C_e}{1 + k_L C_e} \quad (11)$$

18
$$at \ x = \delta, \quad \frac{\partial C_s}{\partial x} = 0 \quad (12)$$

19 Where δ is the maximum penetration depth for the pollutant into the solid phase (m), q_{max} and k_L are the
20 Langmuir constants shown in Tab. 4. The set of partial differential equations was discretized in space in
21 eight nodes along the sorbent thickness (Dorado et al. 2014).

22 The parameter estimation of the different isotherm and kinetic models were solved using MATLAB,
23 minimizing the objective function (OF) given in the equation (13).

$$OF = \sqrt{\sum_{i=1}^N [q(P_1, P_2) - q^*]^2} \quad (13)$$

Where N is the number of measurements realized, q^* is the experimental solute uptake, $q(P_1, P_2)$ is the predicted uptake by the model, P_1 and P_2 are the different estimated parameters. In the case of Langmuir, the parameters are q_{\max} and K_L , for Freundlich K_f and n , for DR q_{\max} and β , for second order k_2 and q_e , for intraparticle K_p and A and for the adsorption diffusion model D and a_s .

6 Results and discussion

7 Activated carbons characterization

The results of elemental analysis, ash and humidity of the three carbons (F-400, NPK and SBC) are listed in Table 2. Data shows that the elemental composition is similar for F-400 and NPK which have high carbon content (about 90%) and differs significantly from those of SBC, which has a carbon content of only 41%. On the other hand, SBC has the highest ash content. High ash content is a common feature of materials prepared from sewage sludge due to the chemical composition and mineral content of this precursor material (Lillo-Rodenas et al. 2008).

Carbons textural properties determined from N_2 adsorption isotherms data are summarized in Table 3. It can be seen that F-400 has the maximum S_{BET} ($1234 \text{ m}^2/\text{g}$), approximately twice as high as those of NPK ($782 \text{ m}^2/\text{g}$), whereas the BET surface area of SBC was, by far, the lowest ($260 \text{ m}^2/\text{g}$). This low BET value of sludge based activated carbon could be attributed to the low carbon content and the high ashes content of their sludge precursor (Anfruns et al. 2011; Smith et al. 2009).

With regards to the adsorption isotherm results (Fig. 1), the F-400 carbon presents the largest nitrogen adsorption followed by the NPK carbon. The N_2 adsorption onto NPK and F-400 takes place, fundamentally, at low relative pressures which is typical of microporous materials. Their isotherms show a gradually upward increase from relative pressures above 0.2, indicating the presence of well-developed mesoporosity. Moreover these isotherms show a hysteresis loop, more important for NPK sample, which is associated to capillary condensation inside the mesopores. The adsorption isotherms present a type I-IV hybrid shape according to the BDDT classification, with a sharp knee at low relative pressures for NPK material suggesting that the microporosity of this sample is mainly composed of pores of a small

1 diameter. The broad knee present in the F-400 isotherm indicates that this carbon has micropore sizes
2 greater than those assigned to NPK. The shapes of hysteresis loops have often been related to specific
3 pore structures. In this respect, the shape of the loop in the nitrogen isotherms of the activated carbons is
4 Type H4, according to the IUPAC nomenclature, which is often associated with narrow slit-like pores. On
5 the other hand, the SBC material shows a small N₂ adsorption capacity with an incipient hysteresis loops.
6 The isotherm belongs to Type I in the BDDT classification, with a clear sharp knee at low relative
7 pressures indicating that the microporosity of this sample is mainly composed of pores of small diameter.

8 The total pore volume values (V_{TOT}) are shown in Table 3. The F-400 exhibits the highest V_{TOT} (0.615
9 cm³/g) whereas the lowest was obtained for SBC (0.161 cm³/g). The pore size distribution was calculated
10 by means of the DFT method and the results are presented in Table 3 and the corresponding plots in Fig.

11 2. An intensive peak at the pore diameter range between 0.6 nm and 0.8 nm can be observed for F-400
12 and NPK carbons (Fig. 2) indicating the presence of narrow micropores or ultramicropores. This is
13 confirmed by the value of ultramicropore volume obtained for these two carbons, ≈ 0.155 cm³/g, (Table
14 3). Nevertheless, the contribution of medium-sized microporosity (0.7 nm-2 nm) is much more important
15 in the F-400 activated carbon (0.221 cm³/g) than in NPK carbon (0,064 cm³/g). In contrast, the activated
16 carbon obtained from sewage sludge presents a low value of both, ultramicropore volume (0.049 cm³/g)
17 and medium-size microporosity (0,023 cm³/g).

18 Regarding mesoporosity, NPK presents the highest mesopore volume (0.120 cm³/g) which is
19 significantly higher than those of F-400 (0.077 cm³/g) and SBC (0.049 cm³/g) carbons.

20 The carbons were also characterized by infrared spectroscopy in order to get information about
21 the main functional groups on the carbons surface. The three IR spectra exhibit a similar profile as can be
22 seen in Fig. 3. However, there are some significant differences among them. In regards to the common
23 bands, the broad band in the 3500-3200 cm⁻¹ region due to O-H stretching vibration can be seen. This
24 band appears in all three recorded spectra, but it is considerably more intense in F-400 and NPK than in
25 SBC. This hydroxyl function could belong to an alcohol, phenol or carboxylic group. However, for F-400
26 spectra, the absence of a peak at approximately 1750-1680 cm⁻¹ characteristic of C=O stretching
27 vibrations rules out the presence of carboxylic group. In contrast, NPK and SBC spectra show a weak
28 band at 1741 cm⁻¹ that indicates the presence of carbonyl function.

1 The two closest and acute bands at 2925 and 2853 cm^{-1} also appear in the three spectra and
2 correspond to asymmetric and symmetric C-H stretching vibrations of aliphatic groups, $-\text{CH}_3$ and $-\text{CH}_2-$.
3 These bands are more intense in the two commercial activated carbons than in the SBC. Their
4 corresponding bending vibrations are observed between 1470 and 1380 cm^{-1} . The overlapped bands at the
5 1585-1650 cm^{-1} region, also common for the three carbons, are due to C=C stretching vibrations in
6 sp^2 hybridized carbons in polyaromatics rings. This band is substantially stronger in F-400 activated
7 carbon than in NPK and exhibits a very low intensity in SBC. An important point of difference between
8 the two commercial activated carbons and SBC appears at 1000-1111 cm^{-1} region cm^{-1} . This strong band,
9 only present in SCB activated carbon spectra, could be attributed to Si-O stretching vibration of mineral
10 matter contained in the carbon (silicates). This result is in agreement with the high ash content found in
11 SCB activated carbon.

12 Adsorption isotherms

13 Adsorption isotherms for atrazine and paracetamol sorption on F-400, NPK and SBC activated carbons
14 are shown in Fig. 4. According to their initial slopes, the NPK and SBC isotherms can be classified as L-
15 type, whereas the F-400 isotherm is H-type according to Giles' classification (Giles et al. 1974a,b). This
16 suggests that F-400 has a high affinity for atrazine and paracetamol.

17 The experimental data were fitted to two-parameter isotherms (Langmuir, Freundlich and
18 Dubinin-Radushkevich). The constants obtained from these three models and the objective function (OF)
19 values are listed in Table 4. According to the OF values, the Langmuir equation provides a better
20 description of the atrazine and paracetamol adsorption onto F-400 and SBC activated carbons, while the
21 Freundlich model explains better the adsorption of these compounds on NPK. DR isotherm shows a lower
22 fitting (higher values of OF) for all the studied cases, indicating this model does not offer a satisfactory
23 description of the experimental behavior. As can be seen from Fig. 4, the NPK experimental isotherm
24 presents two steps: a first step with a short plateau, followed by an increase in the amount of the
25 micropollutant adsorbed and then, a second plateau. This profile, which is more pronounced for atrazine
26 sorption, could be related to the higher mesoporosity of NPK carbon. Konda et al. (2002) showed that the
27 sorption behavior of some organic pesticides on soil could be described by a two-step isotherm and they
28 pointed out that this shape might represent the occurrence of a different type of adsorption mechanism.

1 F-400 exhibits the highest adsorption capacities (q_{\max}) for the two adsorbates (Table 4).
2 Moreover, the higher value of K_L for F-400 compared to those of NPK and SBC indicates that F-400 has
3 a greater affinity for the two contaminants. The different behaviors of the three carbons can be attributed
4 not only to their different surface area but also to their different size pore distribution, functional groups
5 and mineral matter content (Moreno-Castilla 2004; Haydar et al. 2003).

6 To assess the influence of pore size distribution on atrazine and paracetamol adsorption, the
7 maximum adsorption capacities (q_{\max}) were correlated with the meso, micro and ultramicroporous
8 volumes of the three activated carbons (Table 5). As it can be seen, the maximum adsorption capacity
9 (q_{\max}) shows a good linear correlation with the micropore volume values in the 0.7-2 nm width range,
10 suggesting that sorption occurs predominantly in this kind of pores. These results agree with those
11 obtained by other authors studying similar micropollutants sorption on different activated carbons
12 (Moreno-Castilla 2004; Li et al. 2009; Pelekani and Snoeyink 2002). In this sense, the high adsorption of
13 the F-400 carbon could be ascribed to its higher microporous content compared to the other two carbons.
14 The low adsorption capacity of SBC is due to its lower surface area. In addition, the high amount of SBC
15 mineral matter might have a negative effect on the sorption process because mineral matter is able to
16 block the pores of the carbon matrix by adsorbing water due to its hydrophilic character (Moreno-Castilla
17 2004). In this sense, Dorado et al. (2010) observed for the same material (SBC) a decrease of around 60%
18 in the sorption capacity for the organic compounds due to the competition with water for the active sites.
19 However, when comparing the sorption capacity for the same specific surface area, the amount of
20 paracetamol adsorbed per square meter of adsorbent material (0.207 mg/m^2) is higher than that of NPK
21 (0.192 mg/m^2) and even similar to that of F-400 in the case of atrazine (0.175 and 0.172
22 mg/m^2 respectively).

23 When the two compounds adsorptions are compared, it can be seen that paracetamol is more
24 adsorbed than atrazine onto the three activated carbons (Table 4). The adsorption of organic compounds
25 is influenced by different molecular features such as the size, the hydrophobicity and the nature of the
26 functional groups which determine the interaction between the adsorbent and adsorbates (π - π interactions,
27 Hydrogen bonds) (Moreno-Castilla 2004).

28 Although paracetamol is slightly smaller than atrazine, its molecular dimensions are very similar
29 (0.65 nm for paracetamol and 0.72 nm for atrazine) (Rossner et al 2009). Thus, the two molecules are

1 small enough to access the micropores with widths in the 0.7 to 2 nm range. Consequently, the
2 differences found in sorption capacities cannot be attributed to size exclusion effects.

3 It is well known that the nonpolar surface of activated carbons preferably adsorbs hydrophobic
4 compounds with a high octanol/water coefficient (K_{ow}). The K_{ow} may be regarded as an initial indicator
5 of the sorption onto activated carbon (Westerhoff et al. 2005). Mohamed et al. (2011) studied the
6 adsorption of four substituted phenols and concluded that the compound's hydrophobicity is the main
7 factor determining a higher adsorption capacity. The same behavior was observed by Li et al. (2009) for
8 simple aromatic compounds. According to these studies, as atrazine has a higher K_{ow} coefficient than
9 paracetamol (Table 1), a higher adsorption might be expected for atrazine if hydrophobic interactions
10 were the main sorption mechanism. However, in our study paracetamol was more adsorbed than atrazine
11 onto the three carbons. These results are in accordance with the findings of other authors. Pan and Xing
12 (2008) reported no explicit relationship between the sorption constants on carbon nanotubes and K_{ow} for
13 different organic compounds. De Ridder et al. (2010) developed a model to predict equilibrium carbon
14 loading on a specific activated carbon for different solutes that reflected a wide range of solute properties.
15 They concluded that hydrophobic partitioning was the dominant removal mechanism for solutes with \log
16 $K_{ow} > 3.7$. However, solutes with a relative low $\log K_{ow}$ and with groups which are capable of forming
17 H-bonds (such as the compounds tested in the present study) showed higher carbon loading at similar \log
18 K_{ow} values than the solutes without these groups. This means that K_{ow} is not always a determinant factor
19 in adsorption.

20 Several works indicate that the π -stacking interaction between aromatic π -systems in organic
21 compounds and in sorbents is a key mechanism in adsorption processes (Moreno-Castilla 2004;
22 Cotoruelo et al. 2011; Keiluweit and Kleber 2009). Atrazine and paracetamol have different aromatic
23 rings in their structure. Inductive and resonance effects of the substituents affect the charge distribution
24 within aromatic molecules. The $-NHR$ and $-OH$ groups in paracetamol causes an electron density
25 addition to the aromatic ring so that it can act as a π -donor. Conversely, atrazine is a π -deficient N-
26 heterocyclic compound and has a $-Cl$ substituent which is electron-withdrawing. These two features
27 make atrazine a π -acceptor compound. On the other hand, the IR analyses showed that the F-400 and
28 NPK carbons have $-OH$ aromatic groups which increase the electron density of the activated carbon
29 graphitic planes. This makes activated carbon a surface π -donor. It was therefore expected that atrazine

1 (π -electron acceptor) would have more affinity for these activated carbons than paracetamol. However,
2 our experimental results do not support this theory.

3 Another possible mechanism proposed for organic compounds sorption is that based on H-
4 bonding interactions (De Ridder et al. 2010; Moreno-Castilla 2004; Terzik 2000; Villaescusa et al 2011
5 and Welhouse and Bleam 1993). O-H groups present on the surface of the activated carbons can form H-
6 bonds with N-H in Atrazine and O-H in paracetamol. Because OH-OH interactions are more intense than
7 OH-NH interactions, this adsorption mechanism could explain the fact that paracetamol was more
8 adsorbed than atrazine. Furthermore, in the case of atrazine, the steric effect of side-chains might hinder
9 the formation of hydrogen bonds between the molecule and the functional groups of the activated
10 carbons. This proposed mechanism is in agreement with Terzyk 2004 which proposed different
11 adsorption mechanisms for different organic molecules (paracetamol, aniline, phenol and acetanilide)
12 depending on pH conditions. At neutral pH paracetamol was adsorbed via OH group in carbon and carbon
13 modified with NH_3 , and via amide group on modified carbons with acid (H_2SO_4 and HNO_3). On the
14 other hand, the interaction of aniline with surface groups was via weak hydrogen bonds (NH) as
15 suggested by the small value of enthalpy adsorption.

16 Adsorption kinetics

17 A series of kinetic studies was performed to compare the rates of sorption of both organic compounds on
18 the activated carbons F-400, NPK and SBC. The kinetics describes the pollutant uptake, which in turn
19 controls the residence time. This is the key to designing further appropriate sorption treatment processes.
20 Concentration profiles over time are shown in Fig. 5 together with the kinetic models tested. The sorption
21 capacity of the carbons influences the abatement rate since the concentration gradient is the driving force
22 of the process. In this sense, the initial removal rate of both compounds on F-400 is significantly higher
23 than on NPK and much superior to that on SBC. In order to compare the kinetic characteristics of each
24 carbon, the parameters that define the three models tested (pseudo second order, intraparticle diffusion
25 and diffusion-adsorption model) were determined by fitting them to the experimental concentrations
26 measured (Table 6). The OF values indicate the degree of agreement between the model predictions and
27 experimental data. According to the results, the best fitting (the lower OF value) was achieved for the
28 pseudo second order and the diffusion-adsorption models

1 In the case of the pseudo second order model, the k_2 value is proportional to the sorption rate on
2 the materials. An analysis of this parameter shows that, although F-400 and NPK have a higher sorption
3 capacity, the kinetic constant is significantly higher in SBC than in the two other carbons (up to 2.8 and
4 2.3 times higher than F-400 for atrazine and paracetamol, respectively). These results indicate that with
5 its similar sorption capacity, SBC could become an interesting economic alternative by reducing the time
6 required to achieve equilibrium by more than half.

7 An analysis of the results from the intraparticle model, although the model predictions diverge
8 slightly from those of the other models, helps to explain the number of stages that occur in the sorption of
9 each compound (Fig. 6). Whereas three stages were detected in the sorption of atrazine on F-400 and
10 NPK, only two were observed for SBC. Similarly, SBC was one of the carbons with fewest stages in the
11 sorption of paracetamol (three as against the four stages for NPK). It is thought that when there are three
12 stages, the first one corresponds to the external mass transfer, followed by intraparticle diffusion and
13 finally the equilibrium achievement (Ruiz et al 2010). The higher number of stages observed in the NPK
14 carbon illustrate the different behavior of the sorption process through mesoporous and microporous
15 according to the previous characterization of the material.

16 The model developed in the present work, based on the classic diffusion-adsorption reaction
17 models, allows a quantitative comparison of the behavior of different materials by means of only two
18 parameters with physical meaning, in contrast to the previous empirical models. The coefficient diffusion
19 (D) value denotes the relative rate of transfer through the material (i.e. sorption rate) and the effective
20 area (a_s) is the relative amount of area involved in the process. Thus, the most relevant information
21 obtained from this model is that SBC, although it shows the lowest specific surface area, in terms of
22 kinetic behavior has an effective area of the same order of magnitude as F-400 and NPK. In view of the
23 specific surface area of the three materials (Table 6) the percentage of effectiveness was found to be
24 between 11% for F-400 and 50% for SBC.

25 In comparison, for the same carbon and without any exception, the diffusion coefficient of
26 atrazine is always higher than for paracetamol. Although the sorption capacity for atrazine (more
27 hydrophobic) is lower than paracetamol (Table 4), atrazine is adsorbed onto the carbons at a higher rate
28 (and, thus, in a shorter contact time).

29

1 **Conclusions**

2 The characterization of the three activated carbons revealed that F-400 has the highest total microporous
3 volume, containing mainly medium-sized micropores (0.7 nm-2 nm). NPK was found to have the highest
4 mesopore volume whereas its microporosity consists fundamentally of ultramicropores (<0.7 nm). SBC
5 shows low micro and mesoporosity, probably due to its precursor characteristics. F-400 has the highest
6 aromaticity. In contrast, NPK and SBC are richer in carboxylic groups.

7 The Langmuir equation describes the atrazine and paracetamol adsorption onto the F-400 and
8 SBC activated carbons whereas the Freundlich model explains the adsorption of these compounds onto
9 NPK carbon better. The NPK isotherm present two steps and this behavior seems to be related with its
10 higher mesoporosity. F-400 exhibits the highest adsorption capacities and a great affinity for the two
11 adsorbates.

12 Several kinetic models have been used for predicting the uptake rate of emergent
13 contaminants by carbons. The new approach model, presented here, based on diffusion-reaction equations
14 provides the best description of the experimental data. The good agreement with model predictions
15 confirms the feasibility of representing the complex phenomena occurring during sorption by means of
16 relatively simple models. This model provides a powerful predictive tool together with relevant process
17 parameter values (effective area and diffusion coefficient), which allow the characterization and
18 comparison of different materials by means of fitting parameters with physical meaning (e.g. relation
19 between diffusion coefficient and size of pores). Similarly, different surface coatings, carbon activation
20 processes and carbon origins, among others, could be assessed, focusing not only on sorption capacities
21 but also on kinetic limitations. For instance, these kinetic studies have shown SBC to be a promising
22 sorbent material if the specific surface area can be enhanced. The hydrophobic character of the
23 compounds does not show any correlation with the sorption capacities of carbons but it directly relates
24 with the uptake rate, which is a decisive parameter if contact time is a critical factor.

25 Irrespective of the pore structure and surface chemistry, the three activated carbons showed a
26 higher adsorption capacity for paracetamol than for atrazine. Taking into account the characteristics of
27 these compounds, hydrogen bonding is likely to be the main mechanism governing the sorption of the
28 two contaminants.

1 **Acknowledgements**

2 The authors thank the financial support of MICINN (project CTQ 2008-06842-C02-02) and Polytechnic
3 University of Catalonia for supporting Jordi Lladó through a UPC-Doctoral Research Grant.

4 **References**

- 5 Anfruns, A., Martin, M.J., Montes-Moran, M.A., 2011. Removal of odourous VOCs using sludge-based
6 adsorbents. *Chem. Eng. J.* 166, 1022-1031.
- 7 Aworn, A., Thiravetyan, P., Nakbanpote, W., 2009. Preparation of CO₂ activated carbon from corncob
8 for monoethylene glycol adsorption. *Colloid Surf. A-Physicochem Eng. Asp.* 333, 19-25.
- 9 Clark, R.M., 1987. Evaluating the cost and performance of field-scale granular activated carbon systems.
10 *Environ. Sci. Technol.* 21, 573–580.
- 11 Cotoruelo, L.M., Marques, M.D., Leiva, A., Rodriguez-Mirasol, J., Cordero, T. 2011. Adsorption of
12 oxygen-containing aromatics used in petrochemical, pharmaceutical and food industries by means of
13 lignin based active carbons. *Adsorpt.-J Int. Adsorpt. Soc.* 17, 539-550.
- 14 Cutlip, M.B., Shacham, M., 2008. *Problem Solving in Chemical and Biochemical Engineering with*
15 *POLYMATH, EXCEL and MATLAB.* Prentice Hall: New York.
- 16 De Ridder, D.J., Villacorte, L., Verliefde, A.R.D., Verberk, J.Q.J.C., Heijman, S.G.J., Amy, G.L., Van
17 Dijk, J.C., 2010. Modeling equilibrium adsorption of organic micropollutants onto activated carbon.
18 *Water Res.* 44, 3077-3086.
- 19 Dorado, A.D., Gamisans, X., Valderrama, C., Solé, M., Lao, C., 2014. Cr (III) removal from aqueous
20 solutions: A straightforward model approaching of the adsorption in a fixed-bed column. *J. Environ. Sci.*
21 *Health Part A-Toxic/Hazard Subst. Environ. Eng.* 49, 179–186.
- 22 Dorado, A.D., Lafuente, F.J., Gabriel, D., Gamisans, X., 2010. The role of water in the performance of
23 biofilters: Parameterization of pressure drop and sorption capacities for common packing materials. *J.*
24 *Hazard. Mater.* 180, 693-702.
- 25 Giles, C.H., Smith, D., Huitson, A., 1974a. General treatment and classification of solute adsorption-
26 isotherm 1. Theoretical. *J. Colloid Interface Sci.* 47,755-765.
- 27 Giles, C.H., Smith, D., Huitson, A., 1974b. General treatment and classification of solute adsorption-
28 isotherm. 2. Experimental interpretation. *J. Colloid Interface Sci.* 47, 766-778.

1 Haydar, S., Ferro-Garcia, M.A., Rivera-Utrilla, J., Joly, J.P., 2003. Adsorption of p-nitrophenol on an
2 activated carbon with different oxidations. *Carbon* 41, 387-395.

3 Ho, Y.S., McKay, G., 1998. A comparison chemisorption kinetic models applied to pollutant removal on
4 various sorbents. *Process Saf. Environ.* 76,332-340.

5 Keiluweit, M., Kleber, M., 2009. Molecular-level interactions in soils and sediments: the role of aromatic
6 pi-systems. *Environ. Sci. Technol.* 43, 3421-3429.

7 Konda, L.N., Czinkota, I., Fuleky, G., Morovjan, G., 2002. Modeling of single-step and multistep
8 adsorption isotherms of organic pesticides on soil. *J. Agric. Food Chem.* 50, 7326-7331.

9 Li, B., Lei, Z., Huang, Z., 2009. Surface-treated activated carbon for removal of aromatic compounds
10 from water. *Chem. Eng. Technol.* 32, 763-770.

11 Lillo-Rodenas, M.A., Ros, A., Fuente, E., Montes-Moreno, M.A., Martin, M.J., Linares-Solano, A., 2008.
12 Further insights into the activation process of sewage sludge-based precursors by alkaline hydroxides.
13 *Chem. Eng. J.* 142, 168-174.

14 Marsh, H., Rodriguez-Reinoso, F., 2006. *Activated carbon*. Elsevier Science Ltd.

15 Mohamed, E.F., Andriantsiferana, C., Wilhelm, A.M., Delmas, H., 2011. Competitive adsorption of
16 phenolic compounds from aqueous solution using sludge-based activated carbon. *Environ. Technol.* 32,
17 1325-1336.

18 Moreno-Castilla, C., 2004. Adsorption of organic molecules from aqueous solutions on carbon materials.
19 *Carbon* 42, 83-94.

20 Pan, B., Xing, B., 2008. Adsorption Mechanisms of Organic Chemicals on Carbon Nanotubes. *Environ.*
21 *Sci. Technol.* 42, 9005-9013.

22 Pelekani, C., Snoeyink, V.L., 2000. Competitive adsorption between atrazine and methylene blue on
23 activated carbon: the importance of pore size distribution. *Carbon* 38, 1423-1436.

24 Petrovic, M., Gonzalez, S., Barcelo, D., 2003. Analysis and removal of emerging contaminants in
25 wastewater and drinking water. *Trends. Anal. Chem.* 22, 685-696.

26 Rossner, A., Snyder, S.A., Knappe, D.R.U., 2009. Removal of emerging contaminants of concern by
27 alternative adsorbents. *Water Res.* 43, 3787-3796.

28 Ruiz, B., Cabrita, I., Mestre, A.S., Parra, J.B., Pires, J., Carvalho, A.P., Ania, C.O., 2010. Surface
29 heterogeneity effects of activated carbons on the kinetics of paracetamol removal from aqueous solution.
30 *Appl. Surf. Sci.* 256, 5171-5175.

- 1 Schröder, E., Thomauske, K., Oechsler, B., Herberger, S., 2011. Progress in biomass and bioenergy
2 production. Ed Dr. Shahid Shaukat, InTech, 18, 333-356.
- 3 Smith, K.M., Fowler, G.D., Pullket, S., Graham, N.J.D., 2009. Sewage sludge-based adsorbents: A
4 review of their production, properties and use in water treatment applications. *Water Res.* 43, 2569-2594.
- 5 Smith, K.M., Fowler, G.D., 2011. Production of activated carbon from sludge, in Fabregat, A., Bengoa,
6 C., Font, J., Stueber, F. *Reduction, modification and valorization on sludge*, 1st ed. IWA Publishing
7 London, UK, 141-154.
- 8 Terzik, A. P., 2000. The impact of carbon surface composition on the diffusion and adsorption of
9 paracetamol at different temperatures and at the neutral pH. *J. Coll. Interf. Sci.* 230, 219-222.
- 10 Terzik, A.P., 2004. Molecular properties and intermolecular forces – factors balancing the effect of the
11 carbon surface chemistry in adsorption of organic from dilute aqueous solutions. *J. Coll. Interf. Sci.* 275,
12 9-29.
- 13 Villaescusa, I., Fiol, N., Poch, J., Bianchi, A., Bazzicalupi, C., 2011. Mechanism of paracetamol removal
14 by vegetable wastes: The contribution of pi-pi interactions, hydrogen bonding and hydrophobic effect.
15 *Desalination* 270, 135-142.
- 16 Welhouse, G.J., Bleam, W.F., 1993. Cooperative hydrogen bonding of atrazine. *Environ. Sci. Technol.*
17 27, 500-505.
- 18 Westerhoff, P., Yoon, Y., Snyder, S., Wert, E., 2005. Fate of endocrine-disruptor, pharmaceutical, and
19 personal care product chemicals during simulated drinking water treatment processes. *Environ. Sci.*
20 *Technol.* 39, 6649-6663.
- 21 Wolborska, A., 1989. Adsorption on activated carbon of p-nitrophenol from aqueous solution. *Water Res.*
22 23, 85-91
- 23 Yan, G.Y., Viraraghavan, T., Chem, M., 2001. A new model for heavy metal removal in a biosorption
24 column. *Adsorpt. Sci. Technol.* 19, 25-43.

1 **Tables captions**

2 **Table 1.** Physico-chemical properties of atrazine and paracetamol.

3 **Table 2.** Elemental analysis, ash and humidity of the activated carbons.

4 **Table 3.** BET area, total pore volume, ultramicropore, medium-sized micropore, total micropore and
5 mesopore volumes of F-400, NPK and SBC activated carbons.

6 **Table 4.** Isotherm parameters for atrazine and paracetamol sorption on F-400, NPK and SBC.

7 **Table 5.** Coefficient of determination (r^2) for linear regression between maximum sorption capacity
8 (q_{max}) and pore volumes.

9 **Table 6.** Kinetic parameters for atrazine and paracetamol sorption on F-400, NPK and SBC.

10 **Figure captions**

11 **Figure 1** N₂ adsorption isotherms at -196 °C for F-400, NPK and SBC carbons.

12 **Figure 2** Pore size distribution of the activated carbons, obtained by application of the DFT model to the
13 N₂ adsorption data at -196 °C.

14 **Figure 3** IR spectra of SBC, NPK and F-400 carbons.

15 **Figure 4** Experimental data and model predictions for a) atrazine and b) paracetamol adsorption onto the
16 different activated carbons.

17 **Figure 5** Kinetic experimental data and models of a) atrazine, b) paracetamol adsorption onto different
18 activated carbons.

19 **Figure 6** Intraparticle-diffusion plots adsorption of atrazine and paracetamol on the different activated
20 carbons.

Table 1. Physico-chemical properties of atrazine and paracetamol.

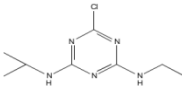
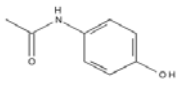
Compound	Atrazine	Paracetamol
Molecular structure		
Molecular formula	$C_8H_{14}ClN_5$	$C_8H_9NO_2$
Molecular weight (g mol ⁻¹)	215.69	151.16
Log K _{ow}	2.43	0.46-0.49
pK _a	2.27	9.86
Molar volume (cm ³ mol ⁻¹)	169.8	120.9

Table 2. Elemental analysis, ash and humidity of the activated carbons.

	F-400	NPK	SBC
Elemental analysis (Dry basis, wt%)			
Carbon	91.00	88.09	41.62
Hydrogen	0.34	0.54	0.62
Nitrogen	1.01	0.88	1.57
Sulfur	0.69	0.24	0.47
Ash	6.92	8.57	55.37
Humidity (wt%)	2.17	5.58	3.97

Table 3. BET area, total pore volume and of ultramicropore, micropore and mesopore of F-400, NPK and SBC activated carbons.

	S_{BET} (m ² /g)	V_{TOT} (cm ³ /g)	V_{umi} (cm ³ /g)	$V_{\text{mi-umi}}$ (cm ³ /g)	V_{mi} (cm ³ /g)	V_{meso} (cm ³ /g)
F-400	1234	0.615	0.154	0.221	0.375	0.077
NPK	782	0.489	0.155	0.064	0.219	0.120
SBC	260	0.161	0.049	0.023	0.073	0.049

Table 4. Isotherm parameters for atrazine and paracetamol sorption on F-400, NPK and SBC.

		Atrazine			Paracetamol		
		F 400	NPK	SBC	F 400	NPK	SBC
Langmuir	q_{\max}	212.26	119.45	45.49	261.04	150.08	53.75
	K_L	0.31	0.09	0.05	0.35	0.06	0.15
	OF	26.79	45.80	9.65	135.10	37.14	12.89
Freundlich	Kt	69.57	22.28	5.99	157.07	28.79	19.04
	n	3.42	2.59	2.23	9.35	3.06	4.69
	OF	44.45	38.65	9.09	138.29	29.57	16.82
DR	β	0.01	0.02	0.13	0.02	0.09	0.015
	q_{\max}	181.76	87.96	32.02	245.18	116.97	45.97
	OF	74.43	63.58	15.09	136.52	68.78	22.54
	E	7.45	4.77	1.93	4.90	2.34	5.87

Table 5. Correlation of determination (r^2) for atrazine and paracetamol sorption capacity (q_{\max}) with pore volume.

	Correlation coefficient (r^2)	
	atrazine	Paracetamol
Ultramicropores (< 0.7 nm)	0.680	0.707
Micropores (0.7-2 nm)	0.934	0.920
Mesopores (2-50 nm)	0.109	0.125

Table 6. Kinetic parameters for atrazine and paracetamol sorption on F-400, NPK and SBC.

		Atrazine			Paracetamol		
		F-400	NPK	SBC	F-400	NPK	SBC
Second order	$k_2 \times 10^{-4}$	1.41	3.50	3.94	1.52	2.16	3.70
	q_e (calc) (mg/g)	195.2	93.55	43.70	190.10	110.30	46.20
	OF	4.69	1.69	1.04	3.31	3.52	1.16
Intraparticle	k_{p1}	1.99	0,61	0,27	1,51	1,03	0,35
	A_1	-7.13	1.06	-0.44	-2.86	-2.86	-1.21
	k_{p2}	1.41	0.31	-4.5×10^{-3}	0.37	0.32	0.21
	A_2	-2.36	7.28	7.05	20.69	6.74	0.54
	k_{p3}	0.13	4.2×10^{-3}	-	0.03	0.61	3.8×10^{-3}
	A_3	28.60	16.19	-	32.99	-1.42	7.79
	k_{p4}	-	-	-	-	1.3×10^{-3}	-
	A_4	-	-	-	-	20.24	-
	OF	7.45	4.83	4.63	8.26	3.84	3.16
Adsorption_diffusion	$D \times 10^{-10}$	7.86	9.29	5.64	7.48	5.90	4.72
	a_s	135.15	112.77	131.34	110.95	109.29	124.75
	OF	4.43	1.48	1.02	3.23	4.15	1.20

